https://doi.org/10.5194/egusphere-2026-2384
Preprint. Discussion started: 8 May 2026

Distribution of cloud geometrical properties and types over the Mediterranean: insights from a decade of CloudSat and 1 year of EarthCARE measurements and ERA5 comparison.

Kalliopi Artemis Voudouri[1,2], Eleni Marinou[1], Iliana Koutsoupi[1,3], Vassilis Spyrakos[1,4], Dimitra Karkani[1], Ioanna Tsikoudi[1,3], Alessandro Battaglia[5], Pavlos Kollias[6], Elina Giannakaki[3], Vassilis Amiridis[1]

[1]National Observatory of Athens, IAASARS, Greece
[2] Department of Physics, Aristotle University of Thessaloniki, Thessaloniki, Greece
[3] Department of Physics, National and Kapodistrian University of Athens, Greece
[4] Laboratory of Atmospheric Physics, Department of Physics, University of Patras, 26500 Rio, Greece
[5]Department of Environment, Land and Infrastructure Engineering, Politecnico di Torino, Turin Italy
[6]School of Marine and Atmospheric Sciences, Stony Brook University, New York, USA

Correspondence to: Kalliopi A. Voudouri (kavoudou@noa.gr)

Abstract. Space-based radar observations from the CloudSat mission are used to characterize cloud properties over the Mediterranean during 2007–2017. CloudSat's Cloud Profiling Radar (CPR) provides vertically resolved cloud measurements, enabling analysis of cloud geometry and type by altitude and month. Low clouds (<1 km a.s.l.) occur up to four times more frequently over sea (32–39%) than land (8–12%). Over land, clouds are most common between 1–4 km, dominated by Stratocumulus (36%), with Altocumulus and Altostratus also present. Over sea, clouds peak at 0–2 km, with Stratocumulus most prevalent, especially in the West Mediterranean. High-level clouds peak at 8–11 km, reaching frequencies of ~30% across the region. Seasonally, Stratocumulus peaks in winter and autumn, while Cumulus maximizes in July–August, particularly in the East Mediterranean. Altostratus and Nimbostratus are least frequent in summer, whereas Altocumulus peaks over East Mediterranean in July–August. High clouds show maxima in spring–early summer and autumn, with minima in midsummer. CloudSat column water and ice are compared with ERA5 reanalysis. Both datasets show similar spatial and seasonal patterns, with higher values over the western and central Mediterranean. Liquid water differences (−0.004 to −0.008 kg/m²) indicate good agreement, while larger ice discrepancies (up to −0.024 ± 0.017 kg/m²) suggest underdetection of thin clouds in ERA5. Preliminary results from the EarthCARE mission are presented but are limited by shorter records. Overall, this study supports improved Climate Data Records and continuity between past, current and future satellite observations.

1 Introduction

Clouds are the primary modulators of the Earth's radiation budget and still constitute the main source of uncertainty in model estimates of climate sensitivity (Randall et al., 2007). The processes governing their formation, evolution, geometrical and microphysical properties, as well as their radiative effects, are still not fully understood (IPCC, 2021). Different cloud types

https://doi.org/10.5194/egusphere-2026-2384
Preprint. Discussion started: 8 May 2026

have different radiative effects, which plays an indispensable role in modulating the global radiative budget. Main knowledge gaps and limitations in current state-of-the-art Global Climate Models (GCMs) are attributed to their inability to correctly describe the ice content in clouds, while the uncertainty is even higher for the quantification of ice and/or water content in Mixed Phase Clouds (Waliser et al., 2009; Komurcu et al., 2014; Barrett et al., 2017; McGraw et al., 2023). These limitations significantly affect the estimation of the cloud albedo in GCMs, altering the equilibrium climate sensitivity according to the different scenarios. Intercomparisons of contemporary climate models further reveal that these uncertainties in cloud ice and mixed-phase processes translate directly into biases in top-of-atmosphere radiative fluxes and cloud feedback diagnostics. The representation of supercooled liquid water, frozen hydrometeor mass, and their vertical distribution remain a primary source of spread in simulated cloud albedo and longwave cloud radiative effects, reinforcing the central role of cloud phase processes in determining model sensitivity to warming (Li, et al., 2023; Cesana et al., 2024). By identifying mixed-phase clouds and their microphysical properties, satellite observations can enhance the characterization of cloud processes and improve model accuracy (Forbes et al., 2016).

State-of-the-art methodologies use combined lidar-radar satellite observations to provide high-resolution vertical profiles of cloud properties and to evaluate or constrain cloud predictions in GCMs. For example, combined CloudSat and CALIPSO (Cloud-Aerosol Lidar and Infrared Pathfinder Satellite Observation) observations provided globally cloud geometrical and microphysical properties from 2006 to 2017 (e.g., Li et al., 2015; raDAR/liDAR product (DARDAR-MASK product); Delanoë et al., 2008). Ceccaldi et al. (2013) developed and validated a synergistic radar–lidar cloud classification algorithm (DARDAR-MASK) that integrates CloudSat and CALIPSO measurements to distinguish cloud phases, including ice, liquid, and mixed-phase categories, demonstrating its utility for detailed cloud phase discrimination and vertical profiling from spaceborne active sensors (Ceccaldi et al., 2013; Delanoë and Hogan, 2010). The recent launch of the ESA's EarthCARE (Cloud, Aerosol and Radiation Explorer) mission, launched on 28 May 2024 (Wehr et al., 2023) is particularly important, as it is foreseen to continue the legacy of CloudSat by extending the global record of cloud observations. It is the largest and most complex Earth Explorer to date and is designed to ensure continuity of the active-sensor cloud record while providing enhanced sensitivity to cloud vertical structure (Feuillard et al., 2026). By extending spaceborne radar-lidar observations, EarthCARE offers improved insight into Mediterranean cloud climatology and strengthens the observational basis needed to evaluate and constrain climate model simulations (Enriquez-Alonso et al., 2016; Sanchez-Lorenzo et al., 2017).

Mediterranean Basin is a climate “hot spot,” characterized by a large variability of cloud systems, ranging from frontal and convective systems to cyclones (Miglietta et al., 2011), and has been the focus of several cloud studies. The study of Raveh-Rubin and Wernli (2015) offers a climatological analysis of large-scale wind and precipitation extremes in the Mediterranean from 1979 to 2012. They identify significant seasonal differences across subregions, with western Mediterranean precipitation extremes being more intense and occurring mainly in autumn, while East Mediterranean events predominantly occur in winter. Chaboureau and Claud (2006) analyzed the climatology of Mediterranean cloud systems and their links to large-scale circulation using data from the TIROS-N Operational Vertical Sounder. They reported that cloud systems are most frequently detected over western North Africa, the eastern coast of Spain, the Balearic Islands, the Gulf of Genoa, southern Italy, the

https://doi.org/10.5194/egusphere-2026-2384
Preprint. Discussion started: 8 May 2026

Aegean Sea, and Cyprus, with peak occurrence between March and October. Ioannidis et al. (2017) examined the seasonal variability of total cloud cover over the Mediterranean during 1948-2014 and identified three dominant modes of seasonal variation. Similarly, Levizzani et al. (2010) produced a 10-year climatology (1996-2005) of warm-season cloud patterns over Europe and the Mediterranean using Meteosat infrared observations.

While these studies have advanced our understanding of cloud occurrence and variability, they rely primarily on passive satellite observations, reanalyses, regional measurements, or overall cloud cover measurements, and therefore lack vertically resolved, long-term information from active sensors (e.g., radar–lidar), leaving gaps in understanding cloud vertical structure and seasonal phase variability across Mediterranean. More recent studies based on ground-based radar observations over selected subregions and limited time periods (e.g., Marinou et al., 2021) have provided detailed regional characterization of cloud types, but their spatial coverage remains restricted. Additionally, few studies have systematically compared multiannual satellite records from active missions such as CloudSat and CALIPSO with outputs from global climate models. Overall, a comprehensive analysis of cloud patterns over the entire Mediterranean region is lacking, especially regarding cloud vertical distributions and seasonal differences.

The aim of this study is threefold. First, we analyze the annual and seasonal vertical distribution of cloud properties across three subregions of the Mediterranean basin using spaceborne radar observations from CloudSat for the period 2007-2017. Second, we compare these observations with the ERA5 reanalysis to evaluate the representation of cloud vertical structure in GCMs. Third, we present recent measurements from the EarthCARE mission, which envisages to ensure observational continuity of CloudSat records while providing enhanced sensitivity to cloud vertical structure.

The paper is structured as follows: Section 2 outlines the methodology used in this study. Section 3 presents the CloudSat statistics (per height and per month), averaged over sea and land for three distinct Mediterranean regions, and the comparison of the cloud patterns derived from CloudSat with those obtained from the ERA5 reanalysis and the EarthCARE's patterns. Finally, Section 4 provides the summary and the main conclusions of the study.

2. Data and Methodology

2.1. Study area

The Mediterranean basin exhibits distinct meteorological regimes across its subregions (Raveh-Rubin and Wernli, 2015 Giuntoli et al., 2022). The West Mediterranean is often affected by convective activity associated with Atlantic weather systems and is characterized by a strong presence of mountains over land. The Central Mediterranean still experiences some deep convective activity, particularly over the sea. This is likely due to the warmer sea surface and the formation of mid-latitude cyclones. On the contrary, the East Mediterranean is dominated by low-level clouds due to the relatively stable and dry atmospheric conditions, especially in summer and autumn.

In this study, the geographical and temporal characterisation of the cloud statistics in the Mediterranean basin [29˚N - 47˚N and 11˚W - 40˚E], is carried out by partitioning the domain in three sub-regions: West [34.9°N - 44.5°N, 5.5°W - 9.2°E],

https://doi.org/10.5194/egusphere-2026-2384
Preprint. Discussion started: 8 May 2026

Central [30.2°N - 45.9°N, 9.2°E - 19.7°E] and East [30.2°N - 41.2°N, 19.7°E - 36.2°E], as shown in Figure 1. Within each region, pixels over land and pixels over ocean are examined separately.

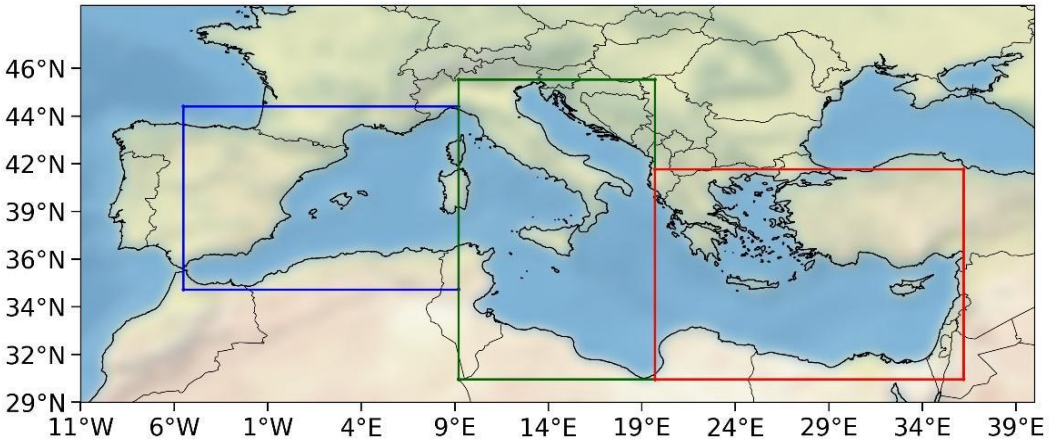

Figure 1: CloudSat data analysis above West (blue), Central (green) and East (red) Mediterranean.

2.2. CloudSat dataset

CloudSat's payload, the Cloud Profiling Radar (CPR) (Stephens et al., 2007, 2008), was the first spacebased 94-GHz (W-band) radar and provided vertical cloud profiles on a global scale. CloudSat was launched on 28 April 2006, and CPR instrument operations began on 2 June 2006. From that time until the end of its operational life (i.e., 20 December 2023), the CPR acquired the first continuous global time series of vertical cloud structure and vertical profiles of cloud liquid water and ice content.

CloudSat flew in the A-Train constellation of satellites. It operated at 94 GHz and had a sensitivity of −30 dBZ. Radar reflectivities were sampled every 240 m and had an effective vertical resolution of approximately 500 m. Profile spacing was about 1 km along track, corresponding to a sampling volume of roughly 1.8 km in the along-track direction and 1.5 km across track. The A-Train constellation was in a Sun-synchronous orbit with equator crossings at approximately 01:30 and 13:30 local time.

In this study we use the following CloudSat dataset (both ascending and descending overpasses): 1) the 2B-GEOPROF (R05) cloud mask and radar reflectivity products (Mace et al., 2006; Marchand et al., 2008), 2) the 2B-CLDCLASS-LIDAR (R05) product is being used for retrieving the heights of the cloud tops and bases and the cloud types (Sassen, K. et al., 2008) and 3) the 2B-CWC-RO (CloudSat Radar-Only Cloud Water Content) (R05) product is being used to retrieve the liquid and ice cloud water path products (Austin et al., 2009). In general, the combination of the CPR and the CALIPSO lidar measurements offer

https://doi.org/10.5194/egusphere-2026-2384
Preprint. Discussion started: 8 May 2026

a more robust cloud type characterization (Sassen et al. 2008; Mace et al. 2009). Using the 'Navigation land sea flag' product, we present the different cloud properties over land and sea.

CloudSat algorithm classified clouds into eight categories: high-level clouds (Cirrus, Cirrostratus; Ci, Cs), altostratus (As), altocumulus (Ac), stratus (St), stratocumulus (Sc), cumulus (Cu), nimbostratus (Ns) and deep convective clouds (Cb). The classification is done based on different rules for hydrometeor vertical and horizontal scales, the maximum Ze measured by the CPR, indications of precipitation, and ancillary data including temperature T profiles and surface topography height (Sassen and Wang, 2007), as predicted by the ERA5 Reanalysis dataset of the European Centre for Medium-Range Weather Forecasts (ECMWF).

The frequency of occurrence of reflectivity values at different heights for all the clouds sampled in each domain is analysed to reveal regional differences in cloud properties, their vertical structure, and precipitation characteristics. Figure 2 shows the Contoured Frequency by Altitude Diagram (CFAD) of the total sample of radar reflectivity analysed in this study. The samples were binned by 1 dBZ at each level and 0.2 km height and were normalized by the total number of profiles at that altitude level. The mean cloud top (~14 km) is noted, as above that, reflectivity values are below the minimum detectable threshold.

Moving downwards through the troposphere, the reflectivity quickly increases. In the upper troposphere (above 8 km), the reflectivity values for the three domains are generally low (-20 to -10 dBZ), indicating the presence of ice clouds or small cloud droplets. In the mid-troposphere (2 - 6 km), higher reflectivity values (~10 dBZ) are found, indicating regions of strong convection. An increase in reflectivity associated with melting is clearly visible between 1 to 2 km a.s.l. Below this, reflectivity increases rapidly towards the surface as the radar signal gets attenuated. The pattern is quite similar in the West and East Mediterranean, with only minor differences observed in the Central.

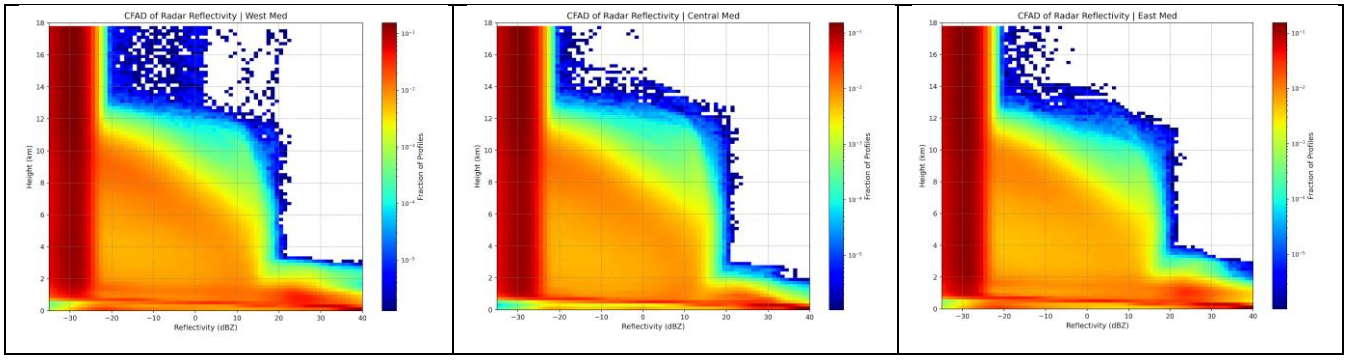

Figure 2: A frequency by altitude diagram (CFAD), showing the frequency of occurrence of values of reflectivity at different heights for the total clouds sampled for West (a), Central (b) and East (c) Mediterranean. Data are binned at 1 dBZ and 0.2 km height and then normalized by the total number of profiles in that height level. The mean cloud top (~14 km) is noted, and above that, reflectivity values are below the minimum detectable threshold.

https://doi.org/10.5194/egusphere-2026-2384
Preprint. Discussion started: 8 May 2026

For the statistical analysis presented below, we used only CloudSat products with high confidence, defined as a CPR_cloud_mask value greater than or equal to 30.

2.3 ERA5 Reanalysis dataset

The ERA5 Reanalysis dataset, produced by the ECMWF/IFS, are available at a horizontal resolution of 0.25° × 0.25° with 137 vertical levels (Vogelezang and Holtslag, 1996), offering a consistent representation of atmospheric conditions. ERA5 has been widely used for climate monitoring, weather analysis, and hydrometeorological studies (Wang et al., 2025). For the purpose of this study, we use hourly values of total column cloud and liquid water from ERA5 reanalyses data, accessed through ECMWF's MARS archive, and regridded through the request on a 1° x 1° spatial resolution. The data can be found in the CDS catalogue: Copernicus Climate Change Service, Climate Data Store, (2023): ERA5 hourly data on single levels from 1940 to present. Copernicus Climate Change Service (C3S) Climate Data Store (CDS). DOI: 10.24381/cds.adbb2d47 (Accessed on 15-09-2025). The datasets are generated using a 4D-Var data assimilation system, that incorporates satellite and in situ observations into the ECMWF Integrated Forecasting System (IFS Cycle 41r2). Hersbach et al. (2020) provide detailed lists and timelines of observation types entering the ERA5 system. The total column liquid and ice water content cloud microphysical properties are used for comparison with CloudSat observations.

2.4 EarthCARE dataset

The Earth Clouds, Aerosols and Radiation Explorer (EarthCARE) mission (Illingworth et al., 2015) carries a CPR operating at 94 GHz (W-band), designed to provide vertically resolved observations of clouds and precipitation with enhanced sensitivity compared to CloudSat. More specifically, the EarthCARE CPR has higher sensitivity (5–6 dB more sensitive), better vertical sampling (100 versus 240 m), higher along-track resolution (500 versus 1100 m) and a smaller instantaneous field of view (IFOV, 800 versus 1400 m) and includes Doppler velocity measurements and improved detection in the lowest atmosphere levels (Mroz et al., 2023). This study utilizes the EarthCARE C-CLD product (Mroz et al., 2023) of BA baseline, with one year of measurements analyzed for the period from October 2024 to October 2025.

3 Results

In this section, we present and analyze the frequency of occurrence of cloud types over the Mediterranean from CloudSat observations, focusing on both their vertical distribution and monthly variability. The analysis spans an 11-year period from January 2007 to December 2017. We further perform a statistical comparison between CloudSat observations and ERA5 outputs, highlighting differences in spatial distribution and cloud water content. Additionally, first-year EarthCARE observations are presented and compared with ERA5, providing an assessment of the continuity of cloud patterns over the region.

https://doi.org/10.5194/egusphere-2026-2384
Preprint. Discussion started: 8 May 2026

3.1. Cloud statistics

The cloud layers distribution over the 3 regions are presented in Figure 3. In most of the cases, single-layer clouds are observed (68-75% of the time), with 20-26% of the cases having double-layer clouds and less than 6% of the cases having three or more cloud layers. A similar number of cloud layers is detected over the West and Central Mediterranean, with higher single-layer clouds observed over the East Mediterranean.

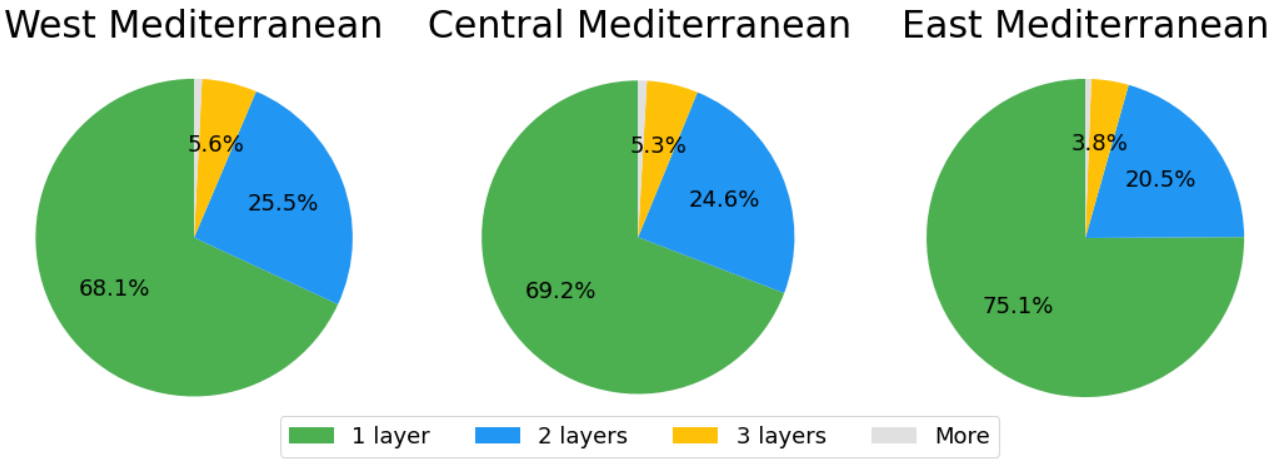

Figure 3. Cloud layers distribution for West (a), Central (b) and East (c) Mediterranean for the period 2007 – 2017.

3.2. Vertical frequency distribution of cloud types

Figure 4 shows the vertical distribution of the different cloud types in the Mediterranean, separated over land (top panel) and sea (lower panel), and over the West (left), Central (center), and East (right) Mediterranean, based on the decadal Cloudsat dataset. All values are divided to the total profile number for each height.

From the statistics, it is evident that the occurrence of low clouds, i.e. below 1 km a.s.l., is almost four times more frequent over sea than over land (32-39 % over sea, 8-12 % over land). In these altitudes, Cu is more frequently observed over sea (in 37 % of the cases), while Sc is more frequently observed over land (in 41 % of the cases). Cu are found with higher percentages over the sea across all regions, with the East Mediterranean showing the highest overall occurrence. Over land, most clouds occur between 1 and 4 km, where Sc clouds are more frequently observed (36 % of the cases), and where Ac and As begin to form. Over sea, most clouds occur between 0-2 km. Stratocumulus are more frequently found over sea than over land across all regions, with the West Mediterranean showing the highest overall occurrence. Stratus is the least frequent category across all regions. As and Ac are the predominant cloud types at altitudes between 4 and 8 km, accounting for 24% of their joint occurrence, while Cirrus (Ci) and Cirrostratus (Cs) are the dominant cloud types at altitudes of 9-11 km over land and 8-11 km over the ocean, accounting for 28% and 33% of occurrences, respectively. High-level clouds (Ci and Cs) show a pronounced peak at 8-11 km across the entire Mediterranean region, with occurrence frequencies reaching up to 30%. Overall,

https://doi.org/10.5194/egusphere-2026-2384
Preprint. Discussion started: 8 May 2026

the presence of high-level clouds over the Mediterranean region is consistent with the global patterns reported by Li et al. (2015). Thick, precipitating stratiform clouds (Ns) are observed mainly in altitudes between 1 to 9 km, at 8% to 19% of the clouds, while thick, rain-bearing deep convective clouds (Cb) represent the second least frequent cloud category over the Mediterranean. They occur more often over the Central Mediterranean (up to about 2%), both over land and sea.

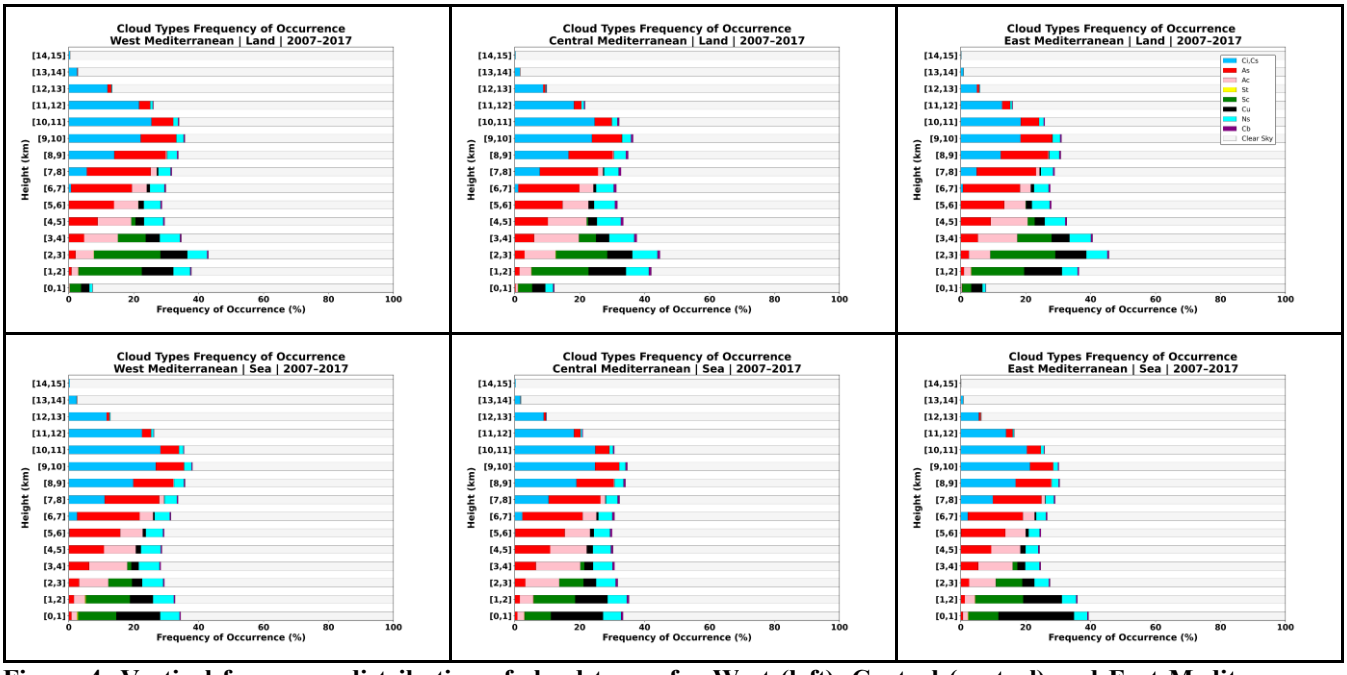

Figure 4: Vertical frequency distribution of cloud types, for West (left), Central (central) and East Mediterranean (right), above Land (up) and Sea (down), during 2007 – 2017.

3.3. Monthly frequency statistics of cloud types

Figure 5 show the monthly frequency statistics of the different cloud types in the Mediterranean region, separated over land (top panel) and sea (lower panel), over the West (left), Central (center), and East (right) Mediterranean, based on the decadal Cloudsat dataset.

Stratocumulus (Sc) exhibits a seasonal pattern, with higher occurrences between January-March and October-December, due to stable marine boundary layer processes. Cumulus (Cu) also exhibits a clear seasonality, with higher occurrences in July and August over both land and sea across all three regions, due to the strong evaporation. Occurrences are particularly high in the East Mediterranean, exceeding 30% over the land and 70% over sea. Altostratus (As) are less frequent in June, July, and August, reaching their lowest percentages in July and August over the East Mediterranean. Altocumulus (Ac) exhibits a different seasonal pattern, with peak occurrences in July and August over the East Mediterranean, over land. Nimbostratus (Ns) shows a minimum between June and September, with near-zero occurrences over the sea in the East Mediterranean. High

https://doi.org/10.5194/egusphere-2026-2384
Preprint. Discussion started: 8 May 2026

clouds (Ci and Cs) exhibit peak frequencies between spring and early summer (April–June) and in autumn (September–October) over both land and sea. Ci and Cs lowest percentages are shown over July and August for the East Mediterranean. The rain-bearing deep convective clouds (Cb) peaks in summer and early autumn over land and for the Central and East Mediterranean.

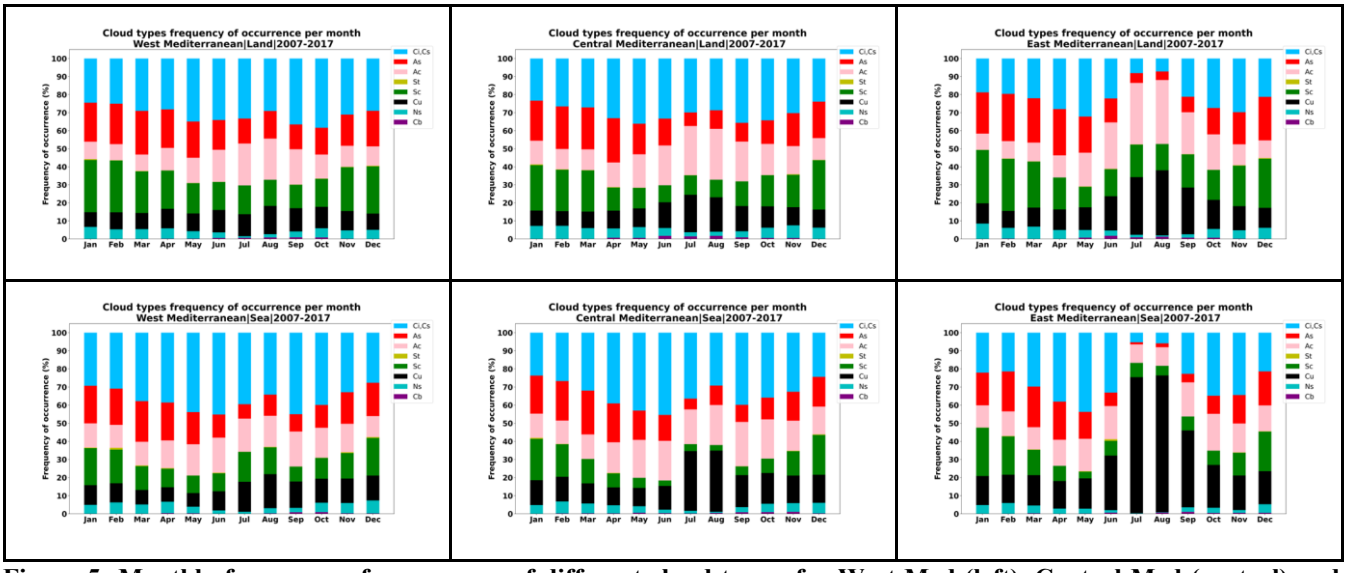

Figure 5: Monthly frequency of occurrence of different cloud types, for West Med (left), Central Med (central) and East Med (left), above Land (up) and Sea (down), for the period 2007 – 2017.

3.4. CloudSat observations vs ERA5 reanalysis: Spatiotemporal patterns

To compare CloudSat with ERA5 and evaluate the reanalysis of cloud predictions, we re-grid CloudSat dataset to the 1° × 1° ERA5 spatial resolution over the Mediterranean domain. Figure 6 presents the mean total column of cloud liquid water (left panels) and cloud ice water (right panels) over the Mediterranean region, based on: (a, b) CloudSat observations, (c, d) ERA5 reanalysis over the full dataset, (e, f) ERA5 reanalysis dataset limited to CloudSat spatiotemporal collocated data and (g, h) the corresponding differences between the ERA5 reanalysis dataset limited to CloudSat spatiotemporal collocated data and the CloudSat dataset.

To handle “problematic” grid cells that exhibited significantly lower counts (or zero counts) compared to their neighboring cells in the collocation process, we defined grid cells with few counts as “empty.” This threshold is considerably lower than the maximum count observed in some cells (approximately 300,000). The values of these low-count (empty) cells were then filled by replacing them with the average of the surrounding cells within a 3 × 3 cell window, with the empty cell at the center. We notice that the ERA5 dataset limited to CloudSat collocated data, captures the same patterns observed in the ERA5 full dataset, although the values are observed noisier. This highlights the representativeness of the Cloudsat decadal climatology to represent the total column cloud liquid/ice water properties in the domain. We observe fair agreement in the regional

https://doi.org/10.5194/egusphere-2026-2384
Preprint. Discussion started: 8 May 2026

distribution of the total column water, with higher values above land, and especially mountainous areas (e.g. Seiki et al., 2019). Total column water is also increased (in both datasets) over northern latitudes.

Overall, the largest deviation from the observations occurs over the sea, with the most significant discrepancy found in the total column of ice water content. More specifically, for total column liquid water, CloudSat values on the ERA5 grid range from 0.038 ± 0.015 kg/m² in the west to 0.029 ± 0.014 kg/m² in the east, while ERA5 collocated with CloudSat reports slightly lower values (0.034 ± 0.020 to 0.022 ± 0.014 kg/m²). The resulting differences (-0.004 to -0.008 kg/m²) indicate good overall agreement between the two datasets. ERA5 systematically underestimates total column ice water compared to CloudSat. While CloudSat on the ERA5 grid reports 0.037 ± 0.015, 0.039 ± 0.022, and 0.029 ± 0.016 kg/m² in the West, Central, and East Mediterranean, respectively, ERA5 collocated with CloudSat shows lower values (0.017 ± 0.004, 0.015 ± 0.008, and 0.012 ± 0.006 kg/m²). The resulting differences (ERA5 - CloudSat) range from -0.017 ± 0.012 to -0.024 ± 0.017 kg/m², with the largest underestimation over the central region. This could be attributed to the fact that many thin clouds are missed or underdetected in the ERA5 reanalysis (Yeo et al., 2022). To the best of our knowledge, this is the first study where the ERA5 cloud properties are evaluated against CloudSat measurements in the Mediterranean region.

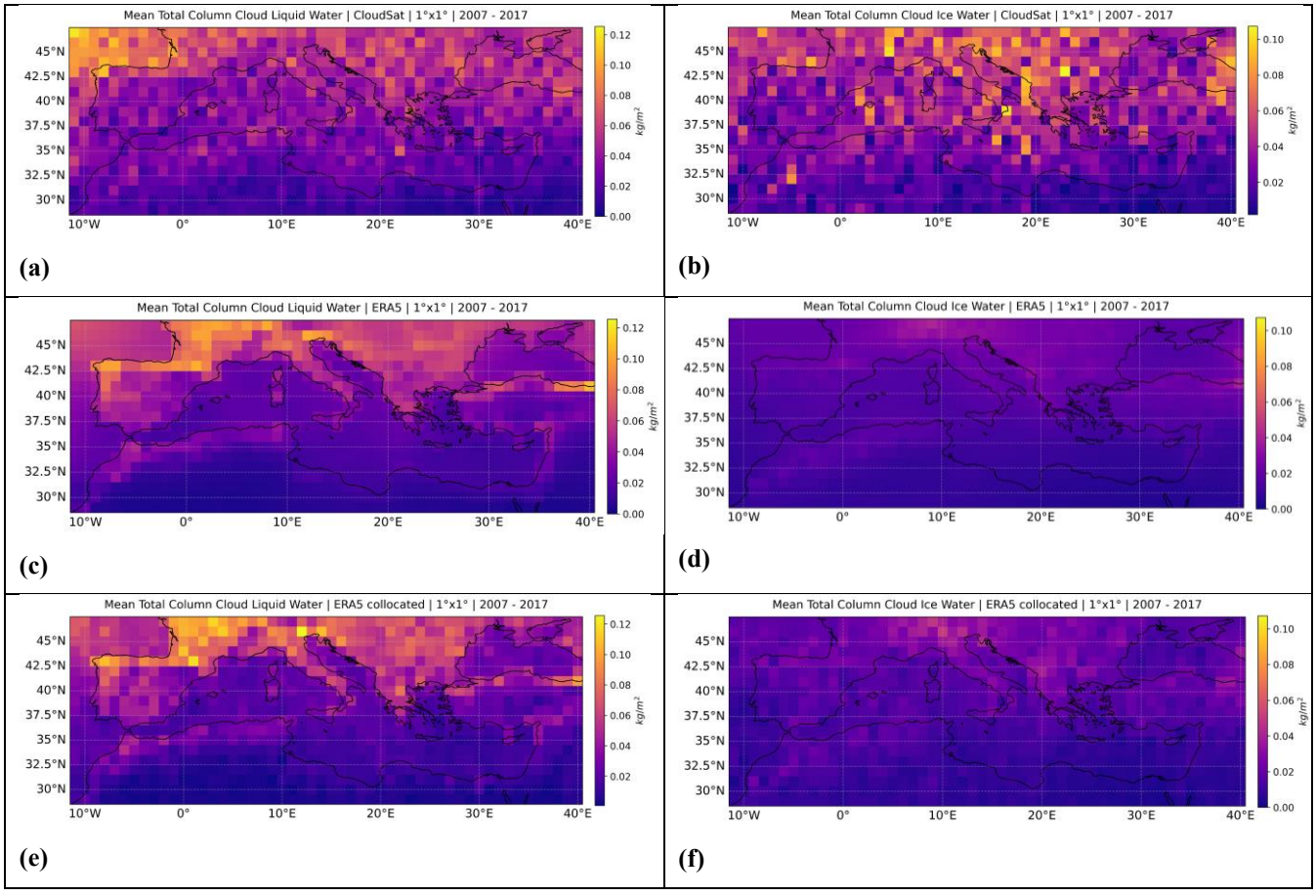

https://doi.org/10.5194/egusphere-2026-2384
Preprint. Discussion started: 8 May 2026

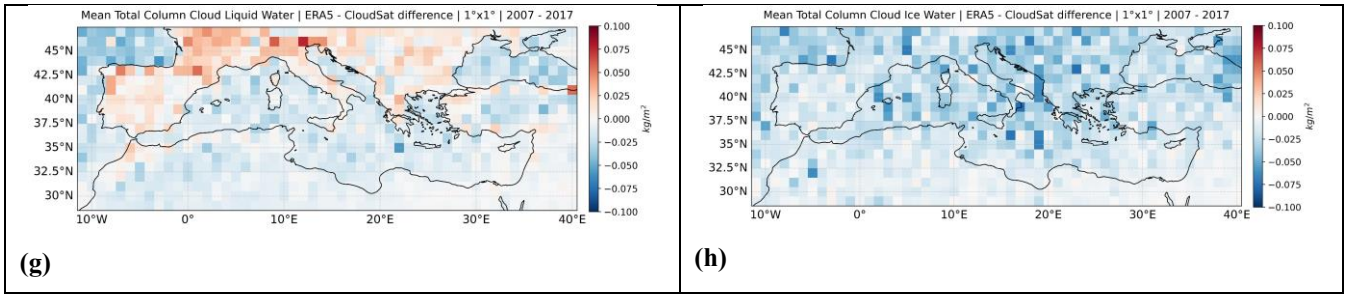

Figure 6. The mean total column cloud liquid water (left panels) and cloud ice water (right panels) over the Mediterranean region derived from CloudSat regridded to ERA5 observations (a, b), the corresponding averages from the ERA5 reanalysis over the full dataset (c, d), the averages from ERA5 sampled only along CloudSat overpasses (e, f) and the corresponding percentage differences between ERA5 and CloudSat (g, h).

A direct comparison between column cloud liquid water (Figure 7a) and cloud ice water (Figure 7b) over the Mediterranean region, between CloudSat regridded to ERA5 and ERA5 sampled along CloudSat observations, is presented below. Figure 7b shows that ERA5 systematically detects lower column ice water values, as indicated by the higher slope. This underestimation could be related to limitations in ERA5 cloud microphysics and vertical resolution (Yeo et al., 2022), which make it difficult to capture thin cirrus layers. In contrast, column liquid water is represented more accurately (Figure 7a), suggesting that ERA5 performs better for low-level clouds than for high-altitude ice clouds.

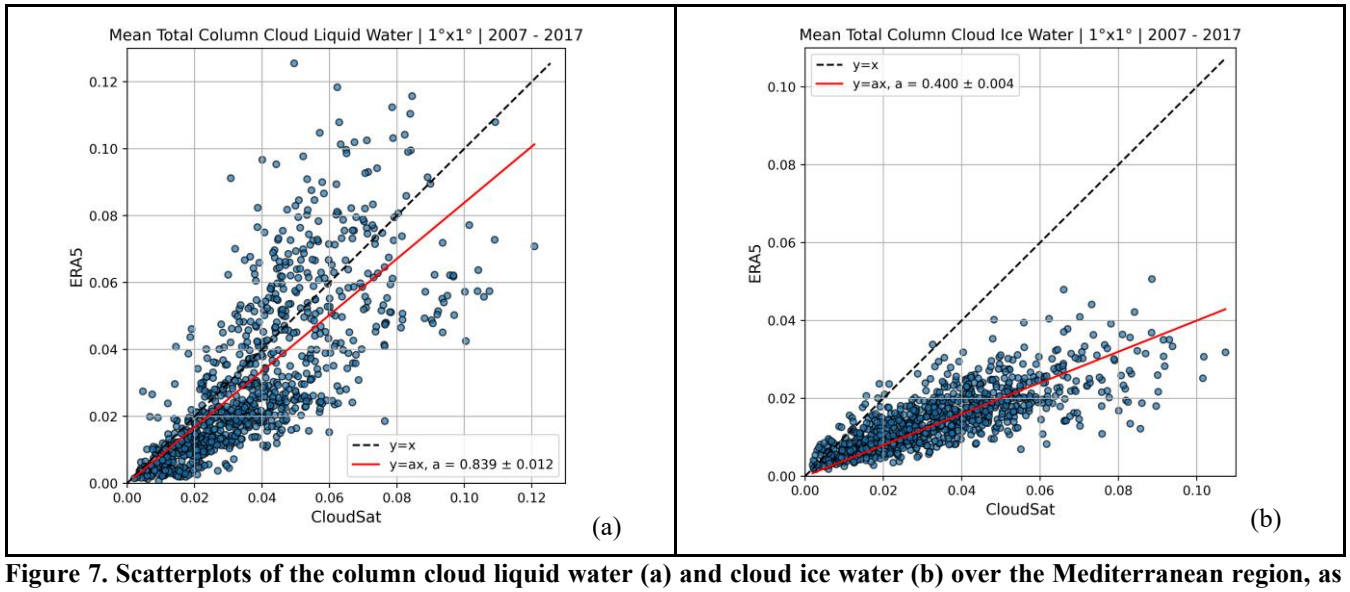

Figure 7. Scatterplots of the column cloud liquid water (a) and cloud ice water (b) over the Mediterranean region, as derived from CloudSat and ERA5 observations.

https://doi.org/10.5194/egusphere-2026-2384
Preprint. Discussion started: 8 May 2026

Figure 8 presents the multiyear annual zonal-mean liquid water path (LWP; blue shading) and ice water path (IWP; brown shading) from (a) CloudSat and (b) the ERA5 dataset, for the overall Mediterranean domain. From Cloudsat, both LWP and IWP exhibit similar patterns, with values increasing toward the northern latitudes. The LWP increases in magnitude as we move towards higher latitudes, while the IWP remains almost stable. Higher IWP and LWP are found in CloudSat observations than in the ERA5 reanalysis dataset (consistent to what is observed in Figure 6). The zonal-mean patterns derived from CloudSat over the Mediterranean in this study are consistent with the global zonal-mean findings of Stephens et al. (2018), although the absolute values differ from their reported statistics. More specifically, Stephens et al. (2018) showed higher annual zonal-mean IWP values, which may be attributed to the different period used (they used the CloudSat 2C-ICE 2006 - 2010 dataset.

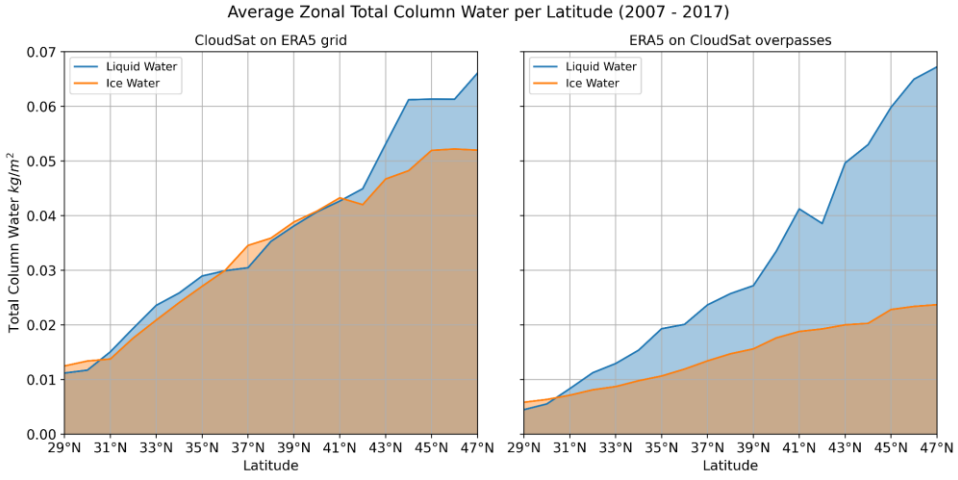

Figure 8: A multiyear annual zonal-mean liquid water path (blue shading) and ice water path (brown shading, from CloudSat 2C-ICE dataset (a) and ERA5 dataset (b) for the period 2007 - 2017.

3.5. CloudSat observations vs ERA5 reanalysis: Monthly patterns

Figure 9 shows the monthly variations of liquid water column (red and orange) and ice (green and blue) and based on CloudSat observations and ERA5 reanalysis, respectively. The results show that ice and liquid water column values are generally higher over land than over sea in both CloudSat and ERA5 datasets. The same monthly pattern is observed in both CloudSat observations and ERA5 modeled fields, with lower values during the summer period (i.e., June, July, August). In general, the East Mediterranean exhibits lower ice and liquid water column values, compared to the other two regions.

More specifically, the CloudSat observations show total column of liquid water values reaching up to 0.055 kg/m², with a significant decrease during the summer period (for all regions), with the minimum value recorded at 0.0057 kg/m² in August over the Eastern Mediterranean. The ERA5 reanalysis shows a similar pattern, with total column liquid water values reaching up to 0.065 kg/m² and exhibiting a comparable decrease during the summer period. Overall, the highest differences between

https://doi.org/10.5194/egusphere-2026-2384
Preprint. Discussion started: 8 May 2026

the Cloudsat and ERA5 collocated datasets is observed in the total column liquid water above the sea (up to 0.043 kg/m² over the Central Mediterranean).

Concerning total column of ice water, CloudSat observations reach up to 0.061 kg/m² over both land and sea in the Central Mediterranean in November. Lower values are consistently found in the ERA5 reanalysis over both land and sea across all months, remaining below 0.03 kg/m².

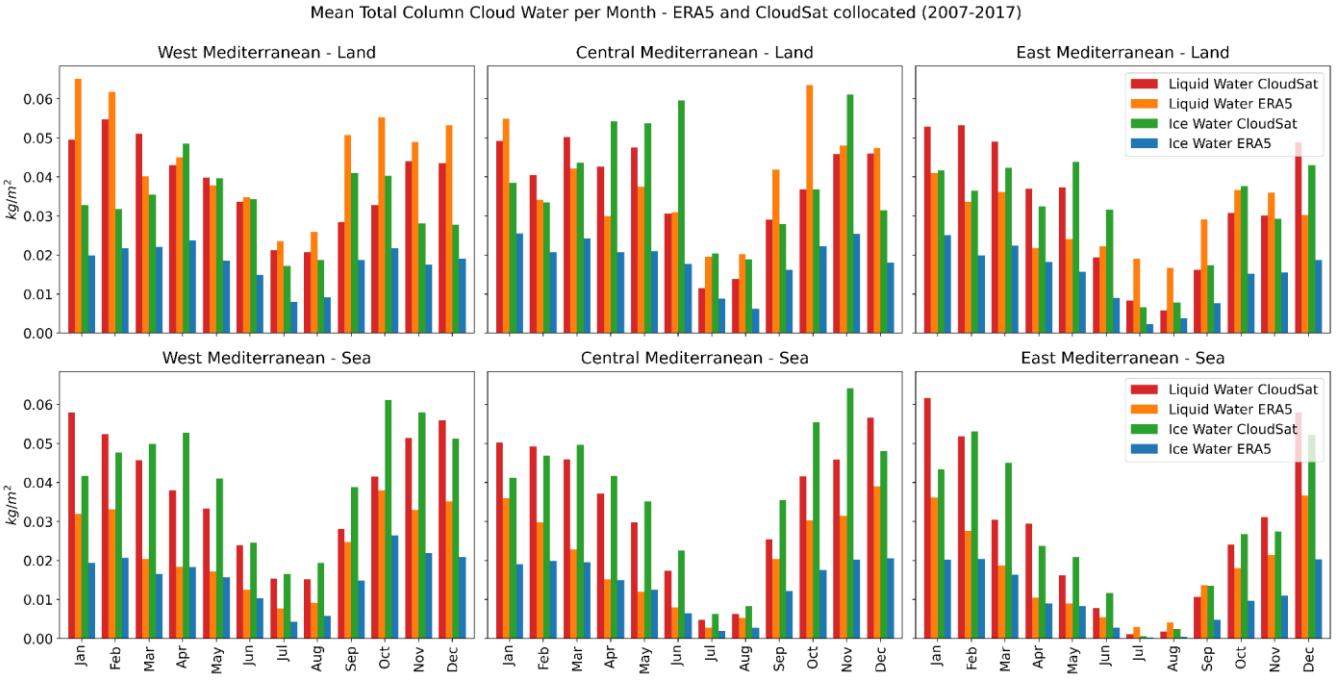

Figure 9: Monthly mean total column of the liquid and ice cloud water, for West Med (left), Central Med (central) and East Med (left), above Land (up) and Sea (down) for the period 2007 – 2017 based on CloudSat and ERA5 observations.

3.6. EarthCARE observations vs ERA5 reanalysis: Seasonal patterns

Figure 10 presents the liquid (blue) and ice (orange) water columns, along with the standard error, derived from the 1 year of EarthCARE observations (October 2024-October 2025). The results show that total column liquid water values are generally higher over land and exceed those retrieved from CloudSat (reaching above 0.7 kg/m² over the East Mediterranean). Similarly, total column ice water values are also higher than the corresponding CloudSat retrievals. The highest value is observed in July, reaching up to 2.7 kg/m² over the Eastern Mediterranean.

It is evident that one year of EarthCARE observations does not capture the monthly patterns observed in the decadal CloudSat statistics. However, it should be noted that additional measurements are needed before drawing robust conclusions.

https://doi.org/10.5194/egusphere-2026-2384
Preprint. Discussion started: 8 May 2026

In general, higher values of both liquid and ice water paths are observed in the one-year EarthCARE dataset. The absolute differences compared to CloudSat can be attributed to the specific meteorological conditions prevailing during the analyzed year, differences in sampling between the two spaceborne radars (e.g., observations at different local times), as well as differences in the applied algorithms.

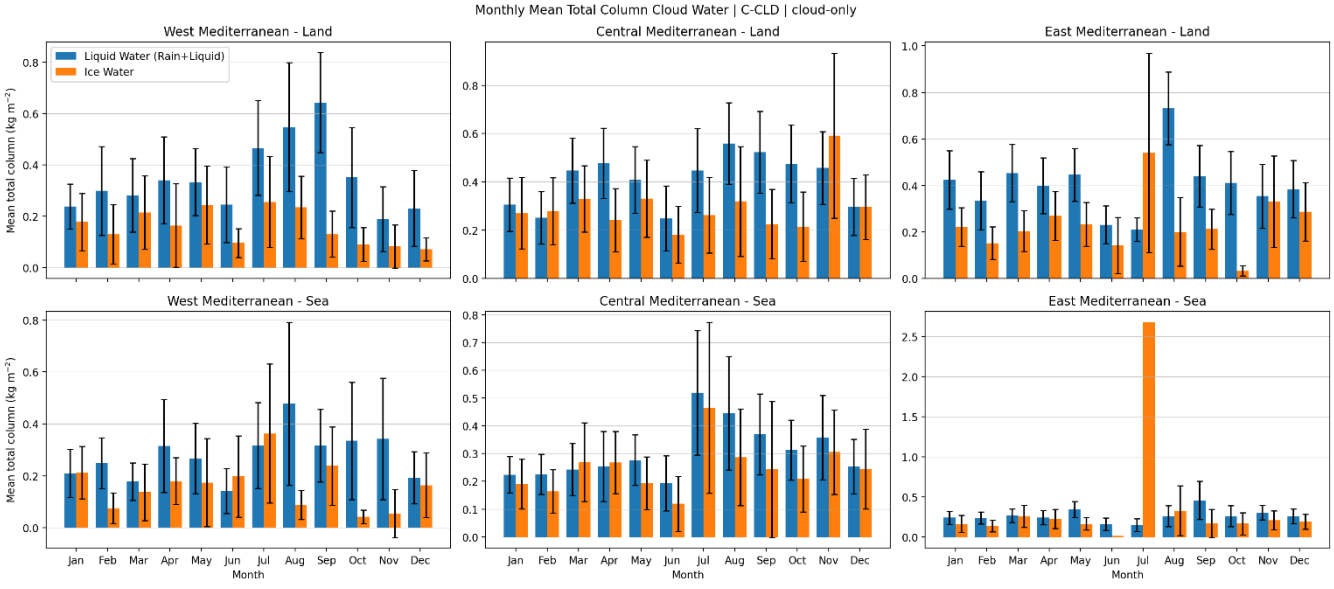

Figure 10: Monthly mean total column of the liquid and ice cloud water, along with the standard error, for West Med (left), Central Med (central) and East Med (left), above Land (up) and Sea (down) for the period 2024 – 2025 based on EarthCARE observations.

A comparison between the one year of EarthCARE observations and ERA5 is also performed. The results are presented on a seasonal basis. Figure 11 illustrates the seasonal variations of liquid (red and orange) and ice water columns (green and blue) based on the 1-year EarthCARE observations and ERA5 reanalysis, respectively. The seasonal patterns indicate that both ice and liquid water column values are generally higher over land than over sea in the EarthCARE and ERA5 datasets, consistent with CloudSat findings from the decadal dataset. However, larger values are found for the 1-year EarthCARE observations. Larger differences are observed in both the ice and liquid water column values over the Central and East Mediterranean, with the highest values generally occurring in the ice water column over land (up to 0.17 kg/m²). These large differences are observed during all seasons. However, a critical factor affecting the reliability of the comparisons is the data availability, therefore, additional measurements will be incorporated in future analyses.

https://doi.org/10.5194/egusphere-2026-2384
Preprint. Discussion started: 8 May 2026

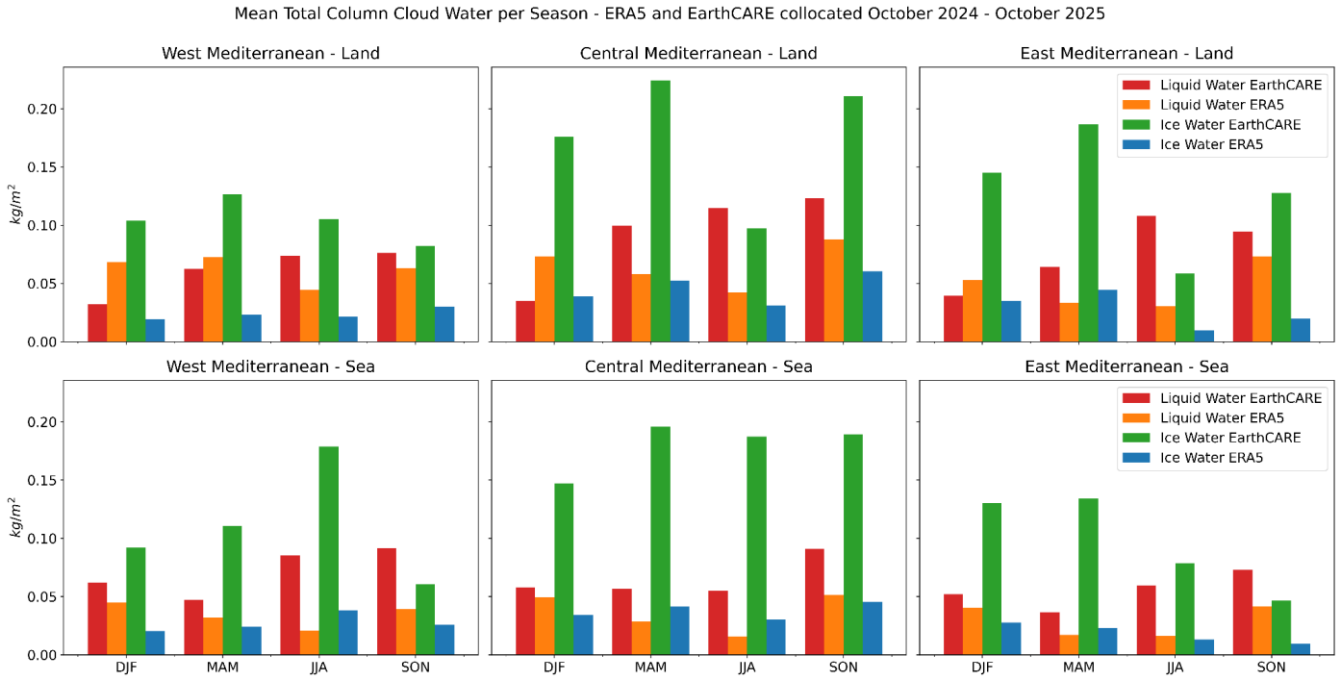

Figure 11: Seasonal mean total column of the liquid and ice cloud water, for West Med (left), Central Med (central) and East Med (left), above Land (up) and Sea (down) for the period October 2024 – October 2025 based on EarthCARE and ERA5 observations.

4 Conclusions

In this study, we examine vertical distributions and patterns of cloud types and properties above the Mediterranean Sea, using a decadal synergistic CloudSat/CALIPSO vertical dataset, and we investigate the capability of ERA5 reanalysis dataset to accurately capture the observed mean IWC and LWC values above the area. In addition, one year of EarthCARE observations is discussed in terms of consistency with the identified monthly patterns. The key findings of this work are summarized below:

- The occurrence of low clouds, with cloud bases below 1 km above the ground, is almost four times more frequent over sea areas compared to land. In this layer, Cu and Sc dominate over sea and land, respectively. Over land, most cloud bases occur between 1 and 3 km, where mid-level clouds (Ac and As) begin to form. They are found with higher percentages over the sea than over land across all regions, with the Central Mediterranean showing the highest overall occurrence. High clouds are common between 6 and 14 km, with a peak at 10-11 km over the entire Med region, with higher percentages over the West and Central Mediterranean (up to 30%). Cb is the less prominent category and more frequent over the central Med (with percentages up to 2%). Over land, deep convective clouds are less frequent but still present, particularly in the West Mediterranean.

https://doi.org/10.5194/egusphere-2026-2384
Preprint. Discussion started: 8 May 2026

- In the West and Central Mediterranean, mid-level clouds (particularly As) are significant in winter and autumn and more frequent over the sea, while low-level clouds are relatively less frequent over land compared to the sea, with peaks in autumn (i.e., October - November) and early winter. Sc dominates above the West Mediterranean during autumn (i.e., September - November) and winter (i.e., December - February), due to stable marine boundary layer processes. The frequency of occurrence of the high clouds above the East Med is low during the summer period and As are less than Ac.
- The comparison of the monthly variations of ice and water columns using CloudSat observations and ERA5 reanalysis show a good agreement in the regional distribution of total column water, with higher values observed over land, particularly in mountainous regions. Total column water is also increased over northern latitudes and mountainous areas. The resulting differences (−0.004 to −0.008 kg/m²) in the liquid water column indicate good overall agreement between the two datasets (ERA5 − CloudSat). In contrast, the differences in the ice water column range from −0.017 ± 0.012 to −0.024 ± 0.017 kg/m², with the largest underestimation occurring over the Central Mediterranean. A number of thin clouds are missing or underdetected in the ERA5 reanalysis dataset.
- The one year of EarthCARE observations of the monthly variations of ice and water columns based on the C-CLD product is also presented. The higher values observed compared to the decadal CloudSat statistics, may be attributed to the specific meteorological conditions prevailing during the analyzed year, differences in the sampling characteristics of the two space-borne radars (including observations at different local times), or discrepancies arising from the applied retrieval algorithms. Future analyses will incorporate additional EarthCARE measurements to evaluate the consistency of liquid and ice water distribution patterns across the Mediterranean region.

The findings of this study can be used to assess cloud microphysical parameterizations in numerical weather prediction (NWP) models, contributing to enhanced forecasts of water and ice. Additionally, the derived statistics on clouds' high-resolution vertical distributions and thermodynamic phase can be combined with the Cloudnet cloud products and lidar-retrieved aerosol properties to study aerosol-cloud interactions in the understudied region of the Mediterranean region. In our future research, we will utilize the full dataset of ESA's Earth Cloud Aerosol and Radiation Explorer (EarthCARE) CPR measurements to derive cloud statistics, aiming to harmonize and bridge past, current and upcoming missions, and to produce Climate Data Records on cloud properties for the Mediterranean region.

Data availability.

The Cloudsat dataset is available at https://cloudsat.atmos.colostate.edu/

ERA5 reanalysis data, accessed from ECMWF's MARS archive, © European Centre for Medium-Range Weather Forecasts (ECMWF), 2025. Licensed under CC-BY-4.0. Dataset available through: Copernicus Climate Change Service, Climate Data Store, (2023): ERA5 hourly data on single levels from 1940 to present. Copernicus Climate Change Service (C3S) Climate Data Store (CDS). DOI: 10.24381/cds.adbb2d47 (Accessed on 15-09-2025).

https://doi.org/10.5194/egusphere-2026-2384
Preprint. Discussion started: 8 May 2026

The EarthCARE Level-2 products (C-FMR and C-CD) used in this study are publicly accessible from the ESA Earth Online gateway at https://earth.esa.int/eogateway/catalog/earthcare-esa-l2-products (last access: 7 November 2025) and via the ESA MAAP where the processing is also conducted. (https://portal.maap.eo.esa.int/)

Author contributions. All authors have contributed to this work. KAV drafted the manuscript and supervised the data processing. EM and AB conceptualized the study. IK and VS processed the CloudSat dataset, while DK and IT handled the EarthCARE dataset. EM, PK, EG, AB and VA reviewed the manuscript.

Competing interests. The authors declare that they have no conflict of interest.

Acknowledgement. This research was supported by PANGEA4CalVal (Grant Agreement 101079201) funded by the European Union, by the EarthCARE DISC project, funded by the European Space Agency under Contract No. 4000144997/24/I-NS and by the Horizon Europe programme under Grant Agreement No 101137680 via project CERTAINTY (Cloud-aERosol inTeractions & their impActs IN The earth sYstem). Part of this work was supported by the COST Action EARLICOST (CA24135), supported by COST (European Cooperation in Science and Technology).

References

Austin, R.T., A.J. Heymsfield, and G. L. Stephens, Retrieval of ice cloud microphysical parameters using the CloudSat millimeter-wave radar and temperature, *J. Geophys. Res.*, 114, D00A23, doi:10.1029/2008JD010049, 2009.

Barrett, Andrew I., Robin J. Hogan, and Richard M. Forbes., Why are mixed-phase altocumulus clouds poorly predicted by large-scale models? Part 1. Physical processes." Journal of Geophysical Research: Atmospheres 122.18 (2017): 9903-9926., 2017.

Battaglia, A., Kollias, P., Dhillon, R., Roy, R., Tanelli, S., Lamer, K., et al., Spaceborne cloud and precipitation radars: Status, challenges, and ways forward. *Reviews of Geophysics*, 58, e2019RG000686. **https://doi.org/10.1029/2019RG000686**, 2020.

Copernicus Climate Change Service, Climate Data Store, (2024): ERA5 post-processed daily-statistics on single levels from 1940 to present. Copernicus Climate Change Service (C3S) Climate Data Store (CDS), DOI: 10.24381/cds.4991cf48 (Accessed on 23-12-2025)

https://doi.org/10.5194/egusphere-2026-2384
Preprint. Discussion started: 8 May 2026

Copernicus Climate Change Service, Climate Data Store, (2023): ERA5 hourly data on single levels from 1940 to present. Copernicus Climate Change Service (C3S) Climate Data Store (CDS). DOI: 10.24381/cds.adbb2d47 (Accessed on 23-12-2025)

Ceccaldi, M., Delanoë, J., Hogan, R. J., Pounder, N. L., Protat, A., From CloudSatCALIPSO to EarthCare: Evolution of the DARDAR cloud classification and its comparison to airborne radar-lidar observations. Journal of Geophysical Research: Atmospheres, 2013, 118 (14), pp.7962- 7981. ff10.1002/jgrd.50579ff, 2013.

Cesana, G.V., Ackerman, A.S., Fridlind, A.M. et al. Observational constraint on a feedback from supercooled clouds reduces projected warming uncertainty. Commun Earth Environ 5, 181 (2024). https://doi.org/10.1038/s43247-024-01339-1

Chaboureau, J.-P., and C. Claud (2006), Satellite-based climatology of Mediterranean cloud systems and their association with large-scale circulation, *J. Geophys. Res.*, 111, D01102, doi:10.1029/2005JD006460, 2006.

Delanoë, J., & Hogan, R. J. A variational scheme for retrieving ice cloud properties from combined radar, lidar, and infrared radiometer. Journal of Geophysical Research, 113, D07204. https://doi.org/10.1029/2007jd009000, 2008.

Delanoë, J., and R. J. Hogan (2010), Combined CloudSat-CALIPSO-MODIS retrievals of the properties of ice clouds, J. Geophys. Res., 115, D00H29, doi:10.1029/2009JD012346.

Engelmann, R., Kanitz, T., Baars, H., Heese, B., Althausen, D., Skupin, A., Wandinger, U., Komppula, M., Stachlewska, I.S., Amiridis, V., et al. The automated multiwavelength Raman polarization and water-vapor lidar PollyXT: The neXT generation. Atmos. Meas. Tech. 9, 1767–1784, 2016.

Enriquez-Alonso, A., Sanchez-Lorenzo, A., Calbó, J. et al. Cloud cover climatologies in the Mediterranean obtained from satellites, surface observations, reanalyses, and CMIP5 simulations: validation and future scenarios. Clim Dyn 47, 249–269, https://doi.org/10.1007/s00382-015-2834-4, 2016.

Feuillard, N., Toledo Bittner, F., Pfitzenmaier, L., Ribaud, J.-F., Delanoë, J., Haeffelin, M., and Dupont, J.-C.: Validation of EarthCARE CPR reflectivity using the ACTRIS cloud radar network, EGUsphere [preprint], https://doi.org/10.5194/egusphere-2026-925, 2026.

Forbes, R., Geer, A., Lonitz, K., Ahlgrimm, M., Reducing systematic errors in cold-air outbreaks, Meteorology section of ECMWF Newsletter No. 146 – Winter 2015/16, pp. 17–22, 2016.

https://doi.org/10.5194/egusphere-2026-2384
Preprint. Discussion started: 8 May 2026

Giuntoli, I., Fabiano, F. & Corti, S. Seasonal predictability of Mediterranean weather regimes in the Copernicus C3S systems. *Clim Dyn* **58**, 2131–2147, https://doi.org/10.1007/s00382-021-05681-4, 2022.

Hersbach H, Bell B, Berrisford P, et al. The ERA5 global reanalysis. *Q J R Meteorol Soc*. 2020; 146: 1999–2049. https://doi.org/10.1002/qj.3803.

Hersbach, H., Bell, B., Berrisford, P., Biavati, G., Horányi, A., Muñoz Sabater, J., Nicolas, J., Peubey, C., Radu, R., Rozum, I., Schepers, D., Simmons, A., Soci, C., Dee, D., Thépaut, J-N. (2023): ERA5 hourly data on single levels from 1940 to present. Copernicus Climate Change Service (C3S) Climate Data Store (CDS), DOI: 10.24381/cds.adbb2d47 (Accessed on 15-09-2025)

Illingworth, A. J., Barker, H. W., Beljaars, A., Ceccaldi, M., Chepfer, H., Clerbaux, N., Cole, J., Delanoë, J., Domenech, C., Donovan, D. P., Fukuda, S., Hirakata, M., Hogan, R. J., Huenerbein, A., Kollias, P., Kubota, T., Nakajima, T., Nakajima, T. Y., Nishizawa, T., Ohno, Y., Okamoto, H., Oki, R., Sato, K., Satoh, M., Shephard, M. W., Velázquez-Blázquez, A., Wandinger, U., Wehr, T., and van Zadelhoff, G.-J.: The EarthCARE Satellite: The Next Step Forward in Global Measurements of Clouds, Aerosols, Precipitation, and Radiation, B. Am. Meteorol. Soc., 96, 1311–1332, https://doi.org/10.1175/BAMS-D-12-00227.1, 2015.

Ioannidis, E., Lolis, C.J., Bartzokas, A., Seasonal Variability of Total Cloud Cover in the Mediterranean Region for the Period 1948–2014. In: Karacostas, T., Bais, A., Nastos, P. (eds) Perspectives on Atmospheric Sciences. Springer Atmospheric Sciences. Springer, Cham. https://doi.org/10.1007/978-3-319-35095-0_89, 2017.

IPCC 2021: Climate Change 2021: The Physical Science Basis. Contribution of Working Group I to the Sixth Assessment Report of the Intergovernmental Panel on Climate Change, edited by: Masson-Delmotte, V., Zhai, P., Pirani, A., Connors, S. L., Péan, C., Berger, S., Caud, N., Chen, Y., Goldfarb, L., Gomis, M. I., Huang, M., Leitzell, K., Lonnoy, E., Matthews, J. B. R., Maycock, T. K., Waterfield, T., Yelekçi, O., Yu, R., and Zhou, B.: Cambridge University Press, Cambridge, United Kingdom and New York, NY, USA, https://doi.org/10.1017/9781009157896, in press, 2021.

Komurcu, M., T. Storelvmo, I. Tan, U. Lohmann, Y. Yun, J. E. Penner, Y. Wang, X. Liu, and T. Takemura, Intercomparison of the cloud water phase among global climate models, J. Geophys. Res. Atmos., 119, 3372–3400, doi:10.1002/2013JD021119, 2014.

Levizzani V., Pinelli F.,Pasqui M., Melani S., Laing AG., Carbone RE, A 10-year climatology of warm-season cloud patterns over Europe and the Mediterranean from Meteosat IR observations, Atmospheric Research 97.4 (2010): 555-576, 2010.

https://doi.org/10.5194/egusphere-2026-2384
Preprint. Discussion started: 8 May 2026

Li, J., Huang, J., Stamnes, K., Wang, T., Lv, Q., and Jin, H.: A global survey of cloud overlap based on CALIPSO and CloudSat measurements, Atmos. Chem. Phys., 15, 519–536, https://doi.org/10.5194/acp-15-519-2015, 2015.

Li, J.-L. F., Xu, K.-M., Tsai, Y.-C., Lee, W.-L., Jiang, J. H., Yu, J.-Y., et al. (2023). Evaluation of radiatively active frozen hydrometeors mass in CMIP6 global climate models using CloudSat-CALIPSO observations. Journal of Geophysical Research: Atmospheres, 128, e2023JD039200. https://doi.org/10.1029/2023JD039200

Mace, G., Marchand, R., Zhang, Q., and Stephens, G. Global hydro-meteor occurrence as observed by CloudSat: Initial observations from summer 2006, Geophys. Res. Lett., 2007, 34, L09808, doi:10.1029/2006GL029017, 2007.

Mace, G. G., Zhang, Y., Marchand, R., Stephens, G., & Ackerman, T., A description of hydrometeor layer occurrence statistics derived from the first year of merged CloudSat and CALIPSO data. Journal of Geophysical Research: Atmospheres, 114(D8), D00A26. https://doi.org/10.1029/2007JD009755, 2009.

Madonna, F., Amodeo, A., Boselli, A., Cornacchia, C., Cuomo, V., D'Amico, G., Giunta, A., Mona, L., Pappalardo, G. CIAO: The CNR-IMAA advanced observatory for atmospheric research. Atmos. Meas. Tech. 4, 1191–1208, 2011.

Marchand, R., G Mace, G, Ackerman, T., and G. Stephens, Hydro-meteor detection using CloudSat an Earth-orbiting 94-GHz cloud radar, J. Atmos. Oceanic Technol., 25(4), 519–533, 2008.

Manninen, A.J., O'Connor, E.J., Vakkari, V., Petäjä, T. A generalised background correction algorithm for a Halo Doppler lidar and its application to data from Finland. Atmos. Meas. Tech. 9, 817–827, 2016.

Marinou, E., Voudouri, K.A., Tsikoudi, I., Drakaki, E., Tsekeri, A., Rosoldi, M., Ene, D., Baars, H., O'Connor, E., Amiridis, V., Meleti, C. Geometrical and Microphysical Properties of Clouds Formed in the Presence of Dust above the Eastern Mediterranean. Remote Sens. 13, 5001. https://doi.org/10.3390/rs13245001, 2021.

McGraw, Z., Storelvmo, T., Polvani, L. M., Hofer, S., Shaw, J. K., & Gettelman, A. (2023). On the links between ice nucleation, cloud phase, and climate sensitivity in CESM2. Geophysical Research Letters, 50, e2023GL105053. https://doi.org/10.1029/2023GL105053

https://doi.org/10.5194/egusphere-2026-2384
Preprint. Discussion started: 8 May 2026

Miglietta MM., Moscatello A., Conte D., Mannarini G., Lacorata G., Rotunno R., Numerical analysis of a Mediterranean 'hurricane' over south-eastern Italy: Sensitivity experiments to sea surface temperature, Atmospheric Research, Volume 101, Issues 1–2, 2011, Pages 412-426, ISSN 0169-8095, https://doi.org/10.1016/j.atmosres.2011.04.006, 2011.

Mroz, K., Treserras, B. P., Battaglia, A., Kollias, P., Tatarevic, A., and Tridon, F.: Cloud and precipitation microphysical retrievals from the EarthCARE Cloud Profiling Radar: the C-CLD product, Atmos. Meas. Tech., 16, 2865–2888, https://doi.org/10.5194/amt-16-2865-2023, 2023.

Nabat, P., Somot, S., Cassou, C., Mallet, M., Michou, M., Bouniol, D., Decharme, B., Drugé, T., Roehrig, R., and Saint-Martin, D.: Modulation of radiative aerosols effects by atmospheric circulation over the Euro-Mediterranean region, Atmos. Chem. Phys., 20, 8315–8349, https://doi.org/10.5194/acp-20-8315-2020, 2020.

Randall, D. A., Wood, R. A., Bony, S., Colman, R., Fichefet, T., Fyfe, J., Kattsov, V., Pitman, A., Shukla, J., Srinivasan, J., Stouffer, R. J., Sumi, A., & Taylor, K. E. (2007). Climate Change 2007: The Physical Science Basis. Contribution of Working Group I to the Fourth Assessment Report of the Intergovernmental Panel on Climate Change (S. Solomon et al., Eds.). Cambridge University Press, 2007.

Raveh-Rubin, S. and Wernli, H., Large-scale wind and precipitation extremes in the Mediterranean: a climatological analysis for 1979–2012. Q.J.R. Meteorol. Soc., 141: 2404-2417. https://doi.org/10.1002/qj.2531, 2015.

Sanchez-Lorenzo, A., Enriquez-Alonso, A., Calbó, J. *et al.* Fewer clouds in the Mediterranean: consistency of observations and climate simulations. *Sci Rep* **7**, 41475, https://doi.org/10.1038/srep41475, 2017.

Sassen, K., Wang, Z., and Liu, D., Global distribution of cirrus clouds from CloudSat/Cloud-Aerosol Lidar and Infrared Pathfinder Satellite Observations (CALIPSO) measurements. *Journal of Geophysical Research: Atmospheres, 113*(D8), D00A12. https://doi.org/10.1029/2008JD009972, 2008.

Sassen, K., and Wang, Z.: Classifying clouds around the globe with the CloudSat radar: 1-year of results, *Geophys. Res. Lett.*, 35, L04805, doi:10.1029/2007GL032591, 2008.

Sassen K., and Wang Z.: Level 2 cloud scenario classification product process description and interface control document, version 5.0, 2007, available at http://cloudsat.cira.colostate.edu/dataICDlist.php?go=list&path=/2B-CLDCLASS.

Seiki, T., Kodama, C., Satoh, M., Hagihara, Y., & Okamoto, H., Characteristics of ice clouds over mountain regions detected by CALIPSO and CloudSat satellite observations. *Journal of Geophysical Research: Atmospheres*, 124, 10858–10877. https://doi.org/10.1029/2019JD030519, 2019.

Stephens, G.L., and N.B. Wood, Properties of Tropical Convection Observed by Millimeter-Wave Radar Systems, *Mon. Wea. Rev.*, *135*, 821-842, doi:10.1175/MWR3321.1, 2007.

Stephens, G.L., D.G. Vane, S. Tanelli, E. Im, S. Durden, M. Rokey, D. Reinke, P. Partain, G.G. Mace, R. Austin, T. L'Ecuyer, J. Haynes, M. Lebsock, K. Suzuki, D. Waliser, D. Wu, J. Kay, A. Gettelman, Z. Wang, and R. Marchand, CloudSat mission: Performance and early science after the first year of operation, *J. Geophys. Res.*, *113*, D00A18, doi:10.1029/2008JD009982, 2008.

Stephens, G., D. Winker, J. Pelon, C. Trepte, D. Vane, C. Yuhas, T. L'Ecuyer, and M. Lebsock, 2018: CloudSat and CALIPSO within the A-Train: Ten Years of Actively Observing the Earth System. Bull. Amer. Meteor. Soc., 99, 569–581, https://doi.org/10.1175/BAMS-D-16-0324.1, 2018.

The PRE-TECT Experimental Campaign. Available online: http://PRE-TECT.space.noa.gr/ (accessed on 25 November 2025).

Vogelezang, D. H. P., and A. A. M. Holtslag, 1996: Evaluation and model impacts of alternative boundary-layer height formulation. *Bound.-Layer Meteor.*, **81**, 245–269, doi:10.1007/BF02430331.

Voudouri, K. A.; Giannakaki, E.; Komppula, M.; and Balis, D. Variability in cirrus cloud properties using a PollyXT Raman lidar over high and tropical latitudes, Atmos. Chem. Phys., 20, 4427–4444, https://doi.org/10.5194/acp-20-4427-2020, 2020.

Waliser, Duane E., et al. "Cloud ice: A climate model challenge with signs and expectations of progress." Journal of Geophysical Research: Atmospheres 114.D8, 2009.

Wang, Z., Bugliaro, L., Gierens, K., Hegglin, M. I., Rohs, S., Petzold, A., Kaufmann, S., and Voigt, C.: Machine learning for improvement of upper-tropospheric relative humidity in ERA5 weather model data, Atmos. Chem. Phys., 25, 2845–2861, https://doi.org/10.5194/acp-25-2845-2025, 2025.

Wehr, T., Kubota, T., Tzeremes, G., Wallace, K., Nakatsuka, H., Ohno, Y., Koopman, R., Rusli, S., Kikuchi, M., Eisinger, M., Tanaka, T., Taga, M., Deghaye, P., Tomita, E., and Bernaerts, D.: The EarthCARE mission – science and system overview, Atmos. Meas. Tech., 16, 3581–3608, https://doi.org/10.5194/amt-16-3581-2023, 2023.

https://doi.org/10.5194/egusphere-2026-2384
Preprint. Discussion started: 8 May 2026

Yeo, H., Kim, M.-H., Son, S.-W., Jeong, J.-H., Yoon, J.-H., Kim, B.-M., and Kim, S.-W.: Arctic cloud properties and associated radiative effects in the three newer reanalysis datasets (ERA5, MERRA-2, JRA-55): Discrepancies and possible causes, Atmospheric Research, Volume 270, 2022, 106080, ISSN 0169-8095, https://doi.org/10.1016/j.atmosres.2022.106080, 2022.